

ADAM PAWEŁ KOZIÓŁ (ORCID: 0000-0002-4059-8639)¹

ADAM KICZKO (ORCID: 0000-0003-0213-2413)¹

MARCIN KRUKOWSKI (ORCID: 0000-0002-4010-7916)¹

GRZEGORZ MAJEWSKI (ORCID: 0000-0002-0122-1409)¹

ANDRZEJ BRANDYK (ORCID: 0000-0002-6021-5340)¹

IDENTIFICATION OF EDDY VISCOSITY PARAMETER AND DEPTH-AVERAGED SECONDARY FLOW IN A COMPOUND CHANNEL WITH AND WITHOUT EMERGED VEGETATION ON FLOODPLAINS

The Shiono–Knight method (SKM) was used to calculate a lateral profile of the depth-averaged velocity and determine the flow rate for a compound channel, both in the presence and absence of emergent vegetation on the floodplains. The SKM is an analytical solution of the Navier–Stokes equations. The effect of vegetation (trees) on flow was simulated using two approaches: with an averaged friction factor and by adding a drag force term in the Navier–Stokes equation. Based on flume and field experiments in compound channels with and without emergent vegetation, values of parameters for the dimensionless eddy viscosity and the secondary flow term were identified using the Monte Carlo sampling technique. The surface of the main channel bed was smooth and made of concrete, whereas the floodplains and all sloping banks were covered by cement mortar composed of terrazzo. Calculations were performed using various models, applied to both laboratory and field data sets. The obtained velocity and flow rate distributions were consistent with observations.

1. INTRODUCTION

Floodplains and riverbanks are usually covered with trees and shrubs. The vegetation has a significant impact on flow conditions in a channel, by increasing flow resistance. It reduces the average velocity, raises water levels in floodplains, and increases the difference between velocities in the main channel and floodplains [1]. Higher veloc-

¹Institute of Environmental Engineering, Warsaw University of Life Sciences, Warsaw, Poland, corresponding author A.P. Koziół, email address: adam_koziol@sggw.edu.pl

ity differences result in strong lateral shear stress, driving a mass and momentum exchange, that affects a stream transport capacity and channel processes. Models for velocity distribution are necessary for channel discharge capacity and also other applications like sediment transport studies. They cannot be elaborated apart from the vegetation effect on the flow, as it is one of the most important factors that shape river flow.

First studies on velocity distributions and flow rates in channels with vegetated and non-vegetated floodplains were performed mostly using laboratory flumes with a smooth bed surface. Knight and Shiono [2] based on extensive laboratory investigations proposed an analytical explanation of the depth-averaged velocity and shear stress distribution in the channel cross-section without vegetation. The literature documents many laboratory and field experiments on the compound channel of a smooth bed with and without emergent vegetation [3–7].

Pasche and Rouve [8] proposed a model for the distribution of the depth-averaged velocity in the channel with vegetated floodplains, derived from Navier–Stokes equations. The model was verified using laboratory measurements. The emergent vegetation effect on the flow was explained using an additional term in Navier–Stokes equations for drag force, exerted by vegetation. Emergent vegetation is often simulated as rigid cylinders, for which dependence between the drag coefficient and Reynolds number is known. For flows past the rigid cylinder with the Reynolds number of 1000, the drag coefficient is around 1.0. Tanino and Nepf [9] showed that for the increasing density of vegetation in the cross-section plane, the value of the drag coefficient reduces as a result of vortex structures generated behind the plant. The effects of vegetation on channel flow have been extensively studied, e.g., by Nepf [10], the influence of trees on the structure of turbulence in a compound open channel in the papers by Sanjou and Nezu [11] and Koziol [1]. The SKM [4] provided an analytical solution for the Navier–Stokes equations concerning velocity, for a channel with vegetation that depends on four parameters: the Darcy–Weisbach friction factor (f) in a channel without vegetation, the dimensionless eddy viscosity (λ), the depth-averaged secondary flow (I) and the bulk drag coefficient (C_D) for vegetation.

These parameters take into account the turbulent interactions, the momentum transfer between the main channel and its floodplains, and the effect of secondary flows, respectively. The friction factor is usually assumed to be constant in each part of the channel, based on experimental results, and back-calculated from calibrated forms the Colebrook–White equation. The calibration range of λ is wide and ranges from 0.005 to 2.5 [12]. To simplify the calibration procedure, a constant value of $\lambda = 0.07$ is often imposed on the whole channel. According to Tang and Knight [5], the variation of λ has a minor effect on the results of the SKM for overbank flows in channels with wide main channels and floodplains, but it has a significant effect for inbank flows. Hence, it is

only the secondary current term, Γ , that requires calibration to model the lateral distribution of streamwise velocity [5]. The calibration range of the secondary current term Γ is wider and ranges from -5 to 5 .

The parameters listed above are especially important in modeling flow rates and velocity distributions in channels of compound cross-sections. Knowledge of the discharge capacity of compound channels is necessary in flood hazard assessments, warning systems, and channel design studies.

The main objective of the present study was an identification of parameters of the eddy viscosity and secondary flows in the analytical model based on the Navier–Stokes equations, accounting for emergent vegetation, described as an additional source of the drag force. Identification of parameters for the Shiono and Knight model, using the Monte Carlo sampling technique, was performed for five tests in a laboratory compound channel, with and without vegetation on the floodplains. In these experiments, the surface of the main channel bed was smooth and made of concrete, whereas the floodplains and all sloping banks were covered by cement mortar composed of terrazzo. Parameter values were also determined for the compound Ihme riverbed, near Hanover, Germany, with the presence of shrubs over the sloping bank of the main channel. Preliminary results for three different experiments were provided by Koziol et al. [13].

2. METHODS AND MATERIALS

2.1. SHIONO AND KNIGHT METHOD (SKM)

Shiono and Knight use a two-dimensional mathematical model to calculate the lateral distribution of the depth-averaged velocities, water flow, and boundary shear stress in laboratory channels [3–7, 14–17] and natural rivers [12, 16, 18].

The SKM is based on a depth-averaged Navier–Stokes equation, expressed for steady flow. The influence of high vegetation was taken into consideration by introducing an additional component to the equation [5]:

$$\underbrace{\frac{\partial(H(\rho UV)_d)}{\partial y}}_I = \underbrace{\rho g H S_0}_{II} - \underbrace{\rho \frac{f}{8} U_d^2 \left(1 + \frac{1}{s^2}\right)^{1/2}}_{III} + \underbrace{\frac{\partial}{\partial y} \left(\rho \lambda H^2 \left(\frac{f}{8}\right)^{1/2} U_d \frac{\partial U_d}{\partial y} \right)}_{IV} - \underbrace{\frac{1}{2\delta} \rho (C_D S_F A_p H)_i}_{V} U_d^2 \quad (1)$$

where: H is the local water depth, $\{U, V\}$ = velocity components in the $\{x, y\}$ directions, x is the streamwise coordinate parallel to the channel bed, y is the lateral coordinate, the subscript d refers to a depth-averaged value, ρ is the fluid density, g is the acceleration

due to gravity, S_0 is the channel bed slope, f – the Darcy–Weisbach friction factor, s is the channel side slope of the banks (1: s , vertical:horizontal), λ is dimensionless eddy viscosity, δ is a porosity, C_D is the drag coefficient, S_F is a shading factor and A_p is the projected area of the vegetation in the streamwise direction per unit volume. The blockage effect of the vegetation is taken into account via a porosity term, δ , where δ is related to the volumetric vegetation density, φ , via $\delta = 1 - \varphi$, where φ is defined as the ratio of the volume of vegetation to the volume of the flow [15]. In Equation (1), term I which includes the lateral and vertical components of velocity is called the secondary flow term (I). Term II is the weight component term. Term III is a component of the friction force determined based on the bed shear stress. Term IV is the resistance component determined based on transverse Reynolds stresses. The last term (V) is the drag force per unit fluid volume due to the vegetation.

Shiono and Knight [4] initially assumed that the secondary flow term $(\partial H(\rho UV)_d / \partial y)$ is zero. Calculated on this assumption the predicted lateral distribution of depth-averaged velocity was in good agreement with the experimental data but the prediction of boundary shear stress was not as good as the prediction of the depth-averaged velocity. Studies have shown that the addition of the secondary flow term made a significant improvement in the prediction of boundary shear stress [19]. Shiono and Knight [4] also demonstrated that, for the particular cases considered, the shear stress term due to secondary flow decreases approximately linearly on either side of a maximum value that occurs at the edge of the floodplain and the main channel. In many solutions of Eq. (1), the secondary flow term $(\partial H(\rho UV)_d / \partial y)$ was expressed as a single parameter Γ . This assumption causes Eq. (1) to become a second-order linear differential equation that can be solved analytically. Equation (1) is most often solved numerically after determining the appropriate boundary conditions in the channel cross-section. The approach used in the SKM is by subdividing the channel cross-section into various subareas (panels) with either constant depth domains or sloping side slope domains, then solving the boundary conditions between adjacent panels and between the edge panels and their boundary, assuming no-slip condition [3]. Three calibration parameters, the Darcy–Weisbach friction factor (f), the dimensionless eddy viscosity (λ), and the secondary flow term (Γ), are required for each panel. In many works, the values of these parameters are given and determined in cross-sections of natural and artificial channels without and with high vegetation [4, 6, 7, 14–16].

For a constant depth panel with vegetation, if C_D , φ , f , λ , Γ are known, the analytical solution of Eq. (1) U_d can be shown to be

$$U_d = \left(A_1 \exp(\gamma y) + A_2 \exp(-\gamma y) + k \right)^{1/2} \quad (2)$$

where unknown constants A_1 and A_2 can be obtained after accepting the appropriate boundary conditions [20]. The values of γ and k are determined from the following equations:

$$\gamma = \left(\frac{2}{\lambda}\right)^{1/2} \left(\frac{f}{8}\right)^{1/4} \frac{1}{H} \left(\frac{f}{8} + \frac{H}{2\delta} C_D S_F A_P\right)^{1/2} \quad (3a)$$

$$k = \frac{gHS_0 - \frac{\Gamma}{\rho}}{\frac{f}{8} + \frac{HC_D S_F A_P}{2\delta}} \quad (3b)$$

For a non-vegetated panel with linearly varying side bed (1:s), U_d can be expressed as:

$$U_d = \left(A_3 \xi^\alpha + A_4 \xi^{-(\alpha+1)} + \omega \xi + \eta\right)^{1/2} \quad (4)$$

The constants A_3 and A_4 are calculated as A_1 and A_2 , ξ is the local depth, and constants α , ω and η are determined from equations:

$$\alpha = -\frac{1}{2} + \frac{1}{2} \left(1 + \frac{s(1+s^2)^{1/2}}{\lambda}\right)^{1/2} (8f)^{1/4} \quad (5a)$$

$$\omega = \frac{gS_0}{\frac{(1+s^2)^{1/2}}{s} \left(\frac{f}{8}\right) - \frac{\lambda}{s^2} \left(\frac{f}{8}\right)^{1/2}} \quad (5b)$$

$$\eta = -\frac{\Gamma}{\rho \frac{f}{8} \frac{(1+s^2)^{1/2}}{s}} \quad (5c)$$

The depth-averaged lateral eddy viscosity ε_{yx} in Eq. (1) is expressed by equations:

$$\varepsilon_{yx} = \lambda H U^* = \lambda H U_d \left(\frac{f}{8}\right)^{1/2}$$

where U^* is shear velocity [5].

The most common way to calculate f is to use the Darcy–Weisbach equation at a known average water flow velocity in a single cross-section or particular parts of the cross-section of a compound channel:

$$f = \frac{8gR_h S_0}{U_i^2} \quad (6)$$

where R_h is the hydraulic radius, U_i – section mean velocity.

With the known Manning roughness coefficient (n) in the cross-section of the channel or its part, the equivalent sand roughness height (k_s) is calculated from the equation [21]:

$$n = \frac{k_s^{1/6}}{8.25g^{1/2}} \quad (7)$$

and then f is calculated from the Colebrook–White equation:

$$f = \left(-2 \log \left(\frac{2.51\nu}{(128gS_0)^{1/2} H^{3/2}} + \frac{k_s}{14.8H} \right) \right)^{-2} \quad (8)$$

where ν is the kinematic viscosity of water.

Calibrated forms of the Colebrook–White equation for the friction factor for smooth channels and vegetated floodplains can be found elsewhere [14]. For smooth channels, f can be calculated from the equation:

$$f = \left(-2 \log \left(\frac{3.02\nu}{(128gS_0)^{1/2} H^{3/2}} + \frac{k_s}{12.3H} \right) \right)^{-2} \quad (9)$$

Vegetation generates turbulence along the entire vertical by creating wake vortices behind it. Additional vortices cause the vertical velocity profile to deviate from a logarithmic distribution. Rameshwaran and Shiono [14] recommended the modified form of the Colebrook–White equation:

$$f = \left(-2 \log \left(\frac{3.02\nu}{(128gH^3S_0)^{1/2}} + \frac{k_s}{1.2H} \right) \right)^{-2} \quad (10)$$

Determination of the values of λ and Γ requires the calibration of the calculation model. The results of the performed hydraulic tests were used to determine the mentioned parameters.

2.2. HYDRAULIC EXPERIMENTS

The measurement data published by Czernuszenko et al. [22], Kozioł [1, 23–25], and Kozioł and Kubrak [26] were used to verify the results of calculations by the SKM. The experiments were carried out in the Hydraulic Laboratory of the Department of Hydraulic Engineering, Faculty of Civil and Environmental Engineering at the Warsaw University of Life Sciences (SGGW). A straight open channel (16 m long and 2.10 m wide) with a symmetrically trapezoidal cross-section was used for the laboratory tests (Fig. 1). The main channel width was 30 cm, and the floodplain width was 60 cm. The

sloping banks were inclined at a slope of 1:1. The channel bed slope of the channel was 0.5%. A uniform and steady flow was used in every case. The water surface was kept parallel to the bed during the experiments. The water surface slope was measured by recording the pressure differences between readings of piezometers located along the centerline of the channel bed at distances of 4 and 12 m from the channel entrance.

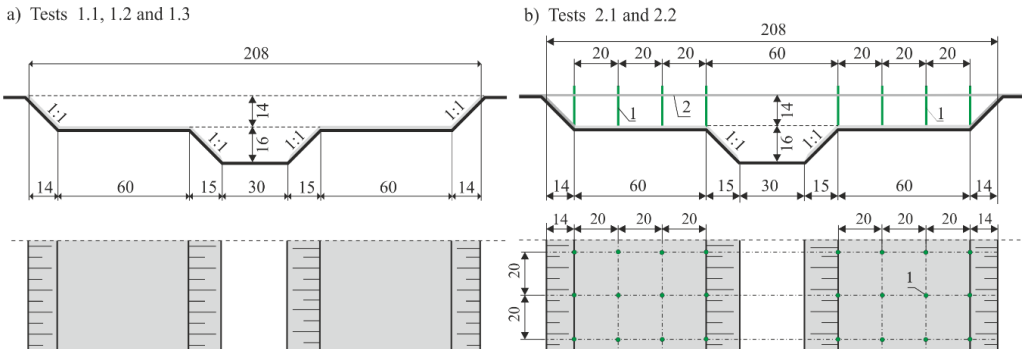


Fig. 1. Scheme of a laboratory cross-section for two considered tests: a) tests 1.1, 1.2, and 1.3 – a channel with a smooth bed and rough sloping banks of the main channel and rough floodplains; b) tests 2.1 and 2.2 in a channel with floodplains vegetated with trees: 1 – aluminum pipes of 0.8 cm diameter imitating trees, 2 – wooden strips supporting the trees (dimensions in cm)

The cross-section halfway down the channel length was selected for velocity measurements. The measurements of instantaneous velocities were carried out at 250 points at 23 verticals – 6 on each floodplain and 11 in the main channel. Instantaneous velocities were measured with the use of a three-component acoustic Doppler velocity meter (ADV) manufactured by Sontek, Inc. The acoustic sensor was mounted on a rigid stem attached to a specially designed trolley allowing its detailed positioning. The measurements were conducted with a maximum frequency of 25 Hz in the velocity range of 0–1.0 m/s with an accuracy of 0.25 cm/s. The measured velocity field was stochastic, therefore it was necessary to test the stationarity and ergodicity of the process. The detailed experimental procedure, such as flow conditions, measurements of instantaneous velocities, and analysis of measurement data sets has been described elsewhere [1].

Five tests for two roughness values of floodplains were conducted. In the first experiment (tests 1.1, 1.2, and 1.3), the surface of the main channel bed was smooth and made of concrete, whereas the floodplains and all sloping banks were covered by cement mortar composed of terrazzo with grains of 0.5–1.0 cm in diameter (Fig. 1a). The surfaces of the floodplains were covered by the same cement mortar with the terrazzo. However, studies showed that calculating the absolute roughness of both surfaces differed due to slight variations in mortar application procedures. The average absolute roughness of the channel surface was determined from the Colebrook–White equation based on the average velocity of the flow measured in those parts of the channel. The

obtained roughness k_s amounted to 0.00005 m for the smooth surfaces, $k_s = 0.0074$ m for the rough surface of the left floodplain, and $k_s = 0.0124$ m for the rough surface of the right floodplain. In the second experiment (tests 2.1 and 2.2), the covering of the floodplains was the same as in the first one, but emergent vegetation (trees) growing on the floodplains were modeled by aluminum pipes of 0.8 cm in diameter, placed with both longitudinal and lateral spacing of 20 cm (Fig. 1b). There were eight pipes in each of 161 cross-sections. The treetops were emergent, and the pipes were not subject to any elastic strains caused by overflowing water. The drag coefficients (C_D) for aluminum pipes were determined from Wieselberger's dependence [27] as a function of the Reynolds number ($Re = U_d D/\nu$, D – pipe diameter). The values of Reynolds numbers ranged from 800 to 8000, therefore the drag coefficient was taken as 1.0. In the experiments conducted for the distributed pipes with the diameter of $D = 0.8$ cm and the density of pipes $33.3/\text{m}^2$, the shading factor S_F was 0.964 and the porosity δ was 0.9983.

The average friction factors in individual sections of the channel section were calculated from Eq. (6) based on the average velocity determined in the tests. The average roughness in the main channel and both floodplains without trees was calculated from Eq. (8), and in floodplains with trees from Eq. (9) based on the average friction factors (Eq. (6)). The roughness of the surface calculated in the main channel was the average value because there were only a smooth bed and rough sloping banks.

3. RESULTS

The SKM [4] was applied to calculate the lateral distribution of the depth-averaged velocity and the flow rate in the compound channel with and without trees in the floodplain (Fig. 1). The cross-section area was divided into three panels (main channel, left and right floodplain) with subareas – 0.05 m wide strips of a constant depth and transverse bed slope. The eddy viscosity and the secondary flow term were identified based on the depth-averaged velocity, measured in laboratory experiments 1.1, 1.2 and 1.3 for smooth main channel bed and rough sloping banks and floodplains and also in experiments with trees in floodplains in the tests 2.1 and 2.2.

In the SKM [4], it is possible to account for channel flow with and without trees in several different ways. Table 1 shows four models used in the study. It was checked which computational model could be used to obtain better compliance of the velocity and flow rate in the channel with the observed values. For the tests without trees models A, B, and C were applied, while for tests including trees A, B, and D ones. In the A model, a constant value of the eddy viscosity coefficient was assumed for the whole channel cross-section and the friction factor in specific channel regions was calculated using Eq. (6) for the mean velocity estimated from measurements. In the test with vegetation, the friction factor was used to describe the flow resistance of trees, and in Eq. (1) $C_D = 0$ was assumed. In contrast to the A, the B model accounts for the variability of

the eddy viscosity in the main channel and floodplains. The eddy viscosity coefficient is assumed to be constant in the C model, where the friction factor is computed based on mean roughness height using Eq. (8) for the main channel and Eq. (9) for the floodplain without trees. In the D model vegetation resistance was described using Eq. (1) with the drag coefficient (C_D), the eddy viscosity coefficient (λ) is assumed to be constant, and the friction factor (f) was calculated with Eqs. (8) and (10) for main channel and floodplain, respectively. Each model was solved for the secondary flow term (Γ) and eddy viscosity coefficient (λ) in the main channel and floodplains. It was assumed that floodplains are symmetric and can be characterized with the same parameter values.

Table 1

Models for the compound channel

Model	Coefficients	Eddy viscosity λ	Equations for calculation f_i
A	$C_D = 0$	$\lambda_{MC} = \lambda_{FP}$	(6)
B		$\lambda_{MC} \neq \lambda_{FP}$	
C		$\lambda_{MC} = \lambda_{FP}$	f_{MC} (8), f_{FP} (9)
D	$C_D = 1, \delta = 0.9983$	$\lambda_{MC} = \lambda_{FP}$	f_{MC} (8), f_{FP} (10)

MC – the main channel, FP – the floodplains.

To solve Eq. (1), the channel cross-section was discretized into panels and subregions. Parameters in the resulting set of equations were identified using Monte Carlo sampling. Eddy viscosity coefficients were uniformly sampled in the range of 0.005–4.5 and the secondary flow values taken from –5 to 5. For various combinations of these two parameters, the velocity distribution and the flow rate were calculated. The best parameter set was selected using the criterion of lowest residuals (difference between measured and calculated values) of the velocity (dU) and flow rate (dQ) (Table 2). The resulting velocity profile along with measured values is provided in Figs. 2 and 3 for the first and second tests, respectively. For the first case (1.1, 1.2 and 1.3 – smooth main channel bed and rough sloping banks and floodplains) there is a good agreement between measured and calculated velocities. The highest differences are present in test 1.3, with the lowest water level, and in the transitional zone between the main channel and the floodplain (Fig. 2). The differences between calculated and observed values of the velocity (dU) were similar in all tests without trees and vary within the range of 0.011–0.020 m/s (2.9–5.3%, Table 2). In the case of the flow rate, relative deviations were in the range of 1.0–1.7% in tests 1.1 and 1.2, reaching around 3% in 1.3 at lower water levels (Table 2). The obtained velocities were almost identical to the measured ones. A slightly better fit was found for the B model, accounting for the variability of the eddy viscosity coefficient. However, the satisfactory results with constant values of this coefficient suggest that its variability can be neglected, as supported by the literature [5, 6, 14–17].

Table 2

SKM model parameters for the tests (trees) and for the River Ihme

Test (Q ; H_{MC})	Model	λ		Γ		dU	dU	dQ	dQ
		MC	FP	MC	FP	[m/s]	[%]	[m ³ /s]	[%]
1.1 (85.2 dm ³ /s; 0.283 m)	A	0.02		0.416	-0.006	0.013	3.3	0.0013	1.3
	B	0.02	0.07	0.416	-0.006	0.013	3.4	0.0010	1.0
	C	0.03		0.527	-0.006	0.012	3.1	0.0015	1.5
1.2 (81.1 dm ³ /s; 0.264 m)	A	0+0.02		0.349	-0.005	0.013	3.6	0.0012	1.4
	B	0.02	0.07	0.362	-0.015	0.013	3.6	0.0010	1.2
	C	0.03		0.453	-0.036	0.012	3.0	0.0014	1.7
1.3 (61.5 dm ³ /s; 0.241 m)	A	0.04		0.272	-0.044	0.020	5.3	0.0017	2.7
	B	0.01	1.01	0.319	-0.075	0.011	2.9	0.0020	3.2
	C	0.03		0.414	-0.075	0.014	3.9	0.0017	2.7
2.1 (trees) (65.7 dm ³ /s; 0.280 m)	A	0.03		0.371	-0.006	0.018	6.5	0.0012	1.8
	B	0.02	0.26	0.384	-0.006	0.015	6.2	0.0008	1.1
	D	0.02		0.851	-0.218	0.014	5.5	0.0009	1.3
2.2 (tress) (58.9 dm ³ /s; 0.263 m)	A	0.03		0.335	-0.005	0.018	8.1	0.0007	1.2
	B	0.01	0.14	0.361	-0.005	0.014	6.2	0.0006	1.0
	D	0.02		0.761	-0.313	0.012	5.1	0.0004	0.7
The River Ihme (shrubs) (207.76 m ³ /s; 4.18 m)	A	0.02		0.159	-0.003	0.109	11.1	-0.914	-0.4

Q – the channel discharge, MC – the main channel, FP – the floodplains. Along the River Ihme, there are bushes over sloping banks of the main channel.

A satisfactory explanation of observations in the first test (1.1, 1.2, and 1.3) was obtained both for averaged-flow resistance coefficients in models A, B, and resistance determined based on the averaged roughness coefficient (k_s) in the C model (Fig. 2). In the main channel of the laboratory flume, the bed roughness is strongly diversified, the bed is smooth and the sloping banks are rough. Modeling attempts, which accounted for this diversification, led to the nonphysical velocity distribution in the cross-section. The main channel is relatively narrow and the roughness of the sloping banks has a much stronger effect on the flow than smooth section of the bed. Therefore, an averaged resistance coefficient (models A and B) or averaged roughness height (k_s as in the C model) provide a better characterization of the hydraulic resistance in the main channel.

In tests 1.1–1.3, the contribution of the secondary flow term (Γ) was noticeably higher in the main channel than in floodplains (Table 2), where they were close to zero. A satisfactory representation of velocity distribution was also obtained by setting Γ equal to zero in the whole channel cross-section, following, i.e., Shiono and Knight [4] and Kubrak and Nachlik [28]. The dimensionless eddy viscosity and the secondary flow term agreed with the literature data for laboratory and field experiments [5, 18]. The results of parameter identification in tests 2.1 and 2.2 are given in Table 2.

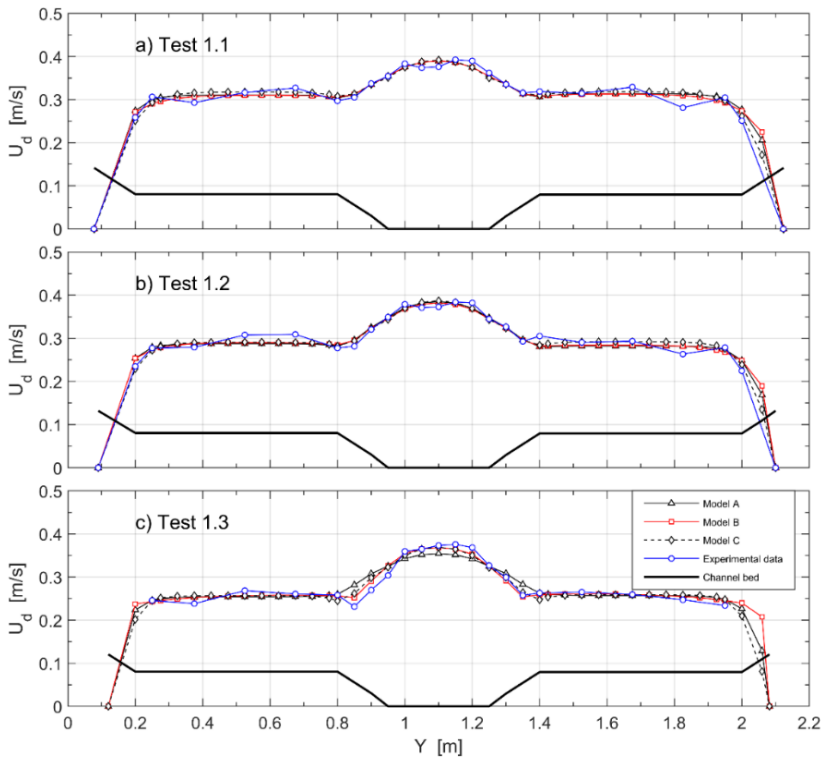


Fig. 2. Calculated and measured velocities U_d in the compound channel in the first tests

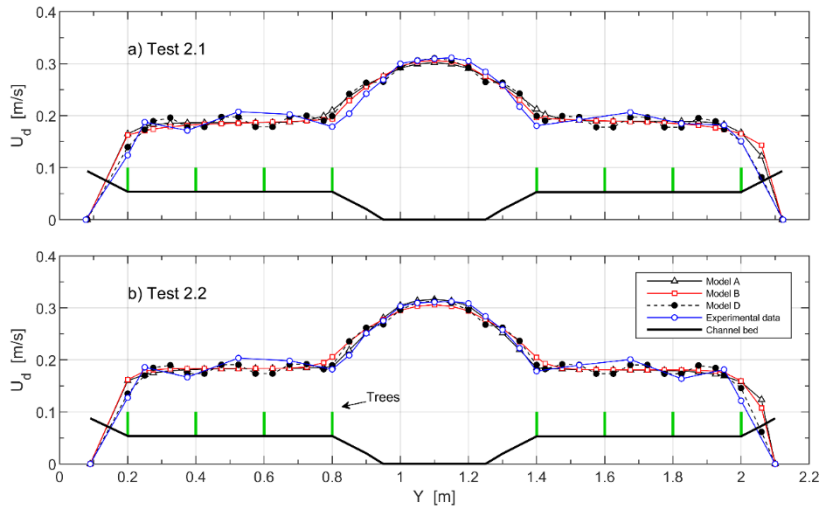


Fig. 3. Calculated and measured velocities U_d in the compound channel in the second test (with trees)

The influence of trees on flow was represented in models A and B with the averaged friction factor (f) and in the D model with drag force term in Eq. (1). Figure 3 shows calculated and measured velocities in tests 2.1 and 2.2. The fits of all applied models: A, B, and D are good, both for velocities in the main channel and floodplains. For the flow in the channel with trees the highest discrepancies between calculated and measured velocities are present in the transitional zone between the main channel and the floodplain (Fig. 3). Model residuals were similar and for the velocity they vary in the range of 0.012–0.018 m/s (5.1–8.1%), while for the flow rate did not exceed 0.0012 m³/s (1.8%, Table 2). The best representation of the process was obtained using the D model, which represents the trees with the drag force term. Modeling the trees with an average friction factor causes flattening of the velocity profile in the floodplain zone (models A and B). The drag term added to the Eq. (1) results in a realistic distribution of the velocity with reduced values behind trees (model D, Fig. 3).

4. DISCUSSION

In all cases values of the secondary flow term (I) were much higher in the main channel than in floodplains (Table 2). Distributions of I were similar in models A and B for both cases, with noticeably bigger levels in tests with trees. The identified eddy viscosities (λ) varied in the range of 0.02–0.04 when assumed uniform in the whole cross-section. For the diversified eddy viscosity between the main channel and the floodplains, values in the main channel were similar to those found previously in the uniform approach. However, in the case of floodplains for flows with higher depth as in tests 1.1 and 1.2, λ increased up to 0.07. In test 1.3 with a lower depth, λ reached even 1.01. In test 2.1 with trees and water levels comparable to those in test 1.1, λ was ca. 0.26, and in the test 2.2 with a lower depth, λ reached even 0.14. The results however support the assumption of a uniform dimensionless eddy viscosity for the whole cross-section because the differences between flow rates in each case were not greater than 1%. Modeling the flow with the averaged value of the friction factor for the resistance induced by trees should be only considered for calculations of flow rates as for sparsely distributed vegetation, the resulting flow profile is non-physically flattened, as showed in Fig. 3 for models A and B in tests 2.1 and 2.2. Accounting for the vegetation drag force in the SKM allowed us to obtain the realistic flow distribution in the cross-section with increased value of the secondary flow term (I) in the main channel and floodplains. Trees in the floodplain increase the longitudinal velocity component, and the longitudinal and the transverse turbulence intensity in the main channel and floodplains [1]. It is expected that the eddy viscosity is higher in vegetated conditions than in non-vegetated ones because the flow passing vegetation produces shedding vortices and turbulence. The three-dimensional studies of turbulence intensity showed an obvious increase in its value in each direction of flow (x , y and z) behind the trees on the floodplains (also in connection

with the main channel) and in the entire main channel [1]. However, in the floodplain results of model B, non-tree test 1.3 is several times larger (1.01) than tree test cases 2.1 and 2.2. At lower relative depths, the spatial flow conditions in the area where the floodplain and the main channel connect change intensively. A physical interpretation of the well-known flow structure in compound flows should be assumed, where for small relative depths (below 0.3) vertical-axis vortices exist in the mixing-layer between the main channel and the floodplains (which should correspond to an increase of the eddy viscosity parameter) and where for higher relative depths the secondary cells (streamwise oriented) should become more pronounced (which should correspond to an increase of the secondary flow parameter). The change in flow structure with flow depth cannot be clearly confirmed due to the small number of measurement cases. There are very few similar studies in the literature (compound channel with emergent vegetation – trees, different bottom roughness) in which parameters calculated based on measurements and relationships prepared depending on the flow conditions are published. The obtained results of the secondary flow term and eddy viscosity coefficients are quite similar in the main channel [5, 16, 29], while they are smaller in the floodplains, which is the result of greater bottom roughness, lower longitudinal velocity, and especially very low transverse velocities.

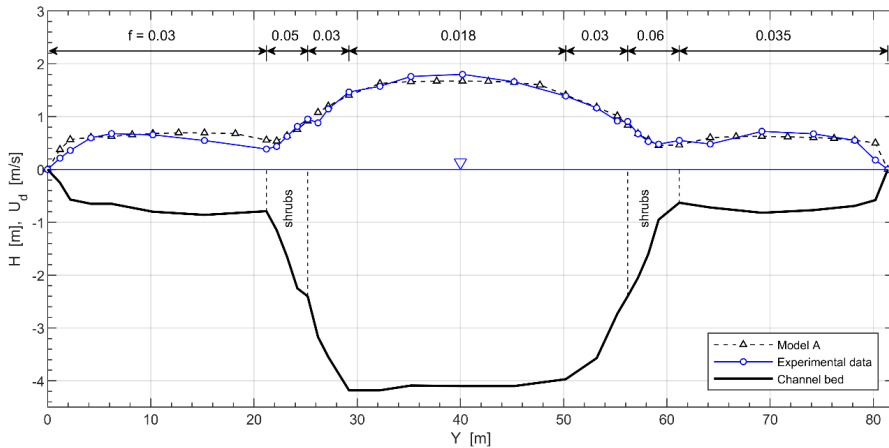


Fig. 4. Predicted U_d and experimental data for the Ihme River

The SKM was also applied for the identification of the dimensionless eddy viscosity and the secondary flow term for the compound cross-section of the Ihme River near Hannover in Germany [30]. Calculations were performed with averaged values of the Darcy–Weisbach friction coefficient for the channel bed surface and shrubs on sloping banks of the main channel. The cross-section of the Ihme River was discretized into three panels and 41 subregions with a constant depth and a transverse slope. The depth averaged velocity profile, obtained using the A model, was very close to the observed

one (Fig. 4). The highest differences were present in the transitional region between the main channel and the left floodplain, what was also reported for this data set by other researchers [11, 14]. The deviation between measured and calculated velocities for the Ihme River is equal 0.109 m/s (11.1%), while in the case of the flow rate, the deviation is ca. 0.914 m³/s (0.4%, Table 2). The values of the secondary flow term (Γ), determined based on observations, were close to these obtained using the A model in analyzed cases, although values of Γ in the main channel were noticeably smaller. Probably, including an additional value of Γ for the vegetation zone in sloping banks of the main channel would allow us to improve the fit of the model's velocity profile. Shrub allocation concentrates on the main channel/floodplain junction. This results in a V-shaped profile of U_d formed around the junction. A similar profile was obtained in the study of Sanjou and Nezu [11] in the case of trees at the floodplain edge. In this case, Model D was not used because the necessary shrub parameters such as the density of shrubs, the shading factor, the porosity, and the drag coefficient were not available.

5. CONCLUSIONS

The SKM enables determining depth average velocity profiles and calculation of flow rates for compound channels with and without vegetation in floodplains. Performed calculations showed that the method provides a satisfactory explanation of laboratory and also field data obtained for the Ihme River. Relative differences between SKM and laboratory measurements did not exceed 3.2%. The highest differences were present at the lowest water levels in a channel. It has been shown that very similar results can be obtained by using different computational models. It was noticed that the best representation of the process was obtained using the model with the drag force term, which represents trees on the floodplains. Modeling of the trees with an average friction factor results in a flattening of the velocity profile in the floodplain zone. However, the additional drag force term results in a realistic velocity distribution with reduced values behind the trees.

The study shows that for the dimensionless eddy viscosity, uniform values can be used for the whole channel cross-section. Separate values for the main channel and floodplains do not significantly improve the explanation of the velocity in the channel with or without trees in the floodplain. The differences in computed flow rates do not exceed 1%.

However, the values of the secondary flow term are different in the main channel and floodplains. In the channel without vegetation, they increase with water depth. In the presence of trees in the floodplain modeled using the average friction factor, the values of the secondary flow term are the same as in the floodplain without vegetation. However, in the main channel, the values are reduced. When the tree effect on flow is

described using the drag force term, apart from the improved representation of velocities, the distribution of values of the secondary flow term is different. Higher values are recorded in the main channel and lower in floodplains.

Calculations showed that in the case of the narrow main channel with rough sloping banks and a smooth bed, rough banks have a much stronger effect on flow. Therefore, an averaged value of the friction factor or the roughness height should be used for the whole main channel.

For the channel cross-section, a uniform value of the dimensionless eddy viscosity can be used at different water depths. In the case of the secondary flow term, different values should be applied in certain parts of the cross-section. Additionally, the values depend on the water depth. Values of the dimensionless eddy viscosity and the secondary flow term, identified in the present study are very close to that provided in the literature for flume and experimental data sets for channels with and without emergent vegetation.

REFERENCES

- [1] KOZIOŁ A.P., *Three-dimensional turbulence intensity in a compound channel*, J. Hydr. Eng., 2013, 139, 852–864. DOI: 10.1061/(ASCE)HY.1943-7900.0000739.
- [2] KNIGHT D.W., SHIONO K., *Turbulence measurements in a shear layer region of a compound channel*, J. Hydr. Res., 1990, 28 (2), 175–196. DOI:10.1080/00221689009499085.
- [3] SHIONO K., KNIGHT D.W., *Mathematical models of flow in two or multi stage straight channels*, Proc. Int. Conf. on River Flood Hydraulics, Wiley, New York 1990, 229–238.
- [4] SHIONO K., KNIGHT D.W., *Turbulent open-channel flows with variable depth across the channel*, J. Fluid Mech., 1991, 222, 617–646. DOI: 10.1017/S0022112091001246.
- [5] TANG X., KNIGHT D.W., *Lateral depth-averaged velocity distributions and bed shear in rectangular compound channels*, J. Hydr. Eng., 2008, 134, 1337–1342. DOI: 10.1061/(ASCE)0733-9429(2008)134:9(1337).
- [6] SHIONO K., TAKEDA M., YANG K., SUGIHARA Y., ISHIGAKI T., *Modeling of vegetated rivers for inbank and overbank flows*, Proc. Int. Conf. on Fluvial Hydraulics: River Flow 2012, September 5–7, San Jose, Costa Rica, 263–269.
- [7] KORDI H., AMINI R., ZAHIRI A., KORDI E., *Practical secondary flow contribution for meandering compound open channels*, ISH J. Hydr. Eng., 2023, 29 (2), 121–128.
- [8] PASCHE E., ROUVÉ G., *Overbank flow with vegetatively roughened flood plains*, J. Hydr. Eng., 1985, 111, 1262–1278. DOI: 10.1061/(ASCE)0733-9429(1985)111:9(1262).
- [9] TANINO Y., NEPF H.M., *Laboratory investigation of mean drag in a random array of rigid, emergent cylinders*, J. Hydr. Eng., 2008, 134 (1), (34). DOI: 10.1061/(ASCE)0733-9429(2008)134:1(34).
- [10] NEPF H.M., *Hydrodynamics of vegetated channels*, J. Hydr. Res., 2012, 50 (3), 262–279. DOI: 10.1080/00221686.2012.696559.
- [11] SANJOU M., NEZU I., *Turbulence structure and concentration exchange property in compound open-channel flows with emergent trees on the floodplain edge*, Int. J. River Basin Manage., 2011, 9 (3–4), 181–193. DOI: 10.1080/15715124.2011.584511.
- [12] SHARIFI S., *Application of evolutionary computation to open channel flow modelling*, University of Birmingham, Birmingham 2009.
- [13] KOZIOŁ A.P., KUBRAK J., KUBRAK E., KRUKOWSKI M., KICZKO A., *Distributions of velocity in compound channels with high vegetation on floodplains*, Acta Sci. Pol. Form. Circ., 2016, 15, 227–241 (in Polish).

- [14] RAMESHWARAN P., SHIONO K., *Quasi two-dimensional model for straight overbank flows through emergent vegetation on floodplains*, J. Hydr. Res., 2007, 45, 302–315. DOI: 10.1080/00221686.2007.9521765.
- [15] TANG X., KNIGHT D.W., *Lateral distributions of streamwise velocity in compound channels with partially vegetated floodplains*, Sci. China, Ser. E, Technol. Sci., 2009, 52, 3357–3362. DOI: 10.1007/s11431-009-0342-7.
- [16] KNIGHT D.W., TANG X., STERLING M., SHIONO K., MCGAHEY C., *Solving open channel flow problems with a simple lateral distribution model*, River Flow, 2010, 1, 41–48.
- [17] SHIONO K., RAMESHWARAN P., *Mathematical modelling of bed shear stress and depth averaged velocity for emergent vegetation on floodplain in compound channel*, e-Proc. 36th IAHR World Congress, 2015, 326–336.
- [18] SHARIFI S., STERLING M., KNIGHT D.W., *Can the application of a multi-objective evolutionary algorithm improve conveyance estimation?*, Water Environ. J., 2011, 25, 230–240. DOI: 10.1111/j.1747-6593.2010.00223.x.
- [19] KNIGHT D.W., YUEN K.W., AL-HAMID A.A., *Boundary shear stress distributions in open channel flow*, [In:] K.J. Beven, P.C. Chatwin, J.H. Millibank (Eds.), *Mixing and Transport in the Environment*, John Wiley & Sons, 1994, 51–87.
- [20] KNIGHT D.W., OMRAN M., TANG X., *Modeling depth-averaged velocity and boundary shear*, J. Hydr. Eng., 2007, 133, 39–47.
- [21] ACKERS P., *Hydraulic design of straight compound channels*, Vol. 1. *Summary and Design Method*, Vol. 2. *Appendices*, Hydraulics Research Limited, Wallington, UK, 1991.
- [22] CZERNUSZENKO W., KOZIOL A.P., ROWIŃSKI P.M., *Measurements of 3D turbulent structure in a compound channel*, Arch. Hydro-Eng. Environ. Mech., 2007, 51, 3–21.
- [23] KOZIOL A.P., *Investigation of the time and spatial macro-scale of turbulence in a compound channel*, Acta Sci. Pol. Arch., 2008, 7, 15–23 (in Polish).
- [24] KOZIOL A.P., *Turbulent kinetic energy of water in a compound channel*, Ann. Warsaw Univ. Life Sci. – SGGW, L. Reclam., 2011, 43, 193–205.
- [25] KOZIOL A.P., *Scales of turbulent eddies in a compound channel*, Acta Geophys., 2015, 63, 514–532. DOI: 10.2478/s11600-014-0247-0.
- [26] KOZIOL A.P., KUBRAK J., *Measurements of turbulence structure in a compound channel*, [In:] P. Rowiński, A. Radecki-Pawlik (Eds.), *Rivers – Physical, Fluvial and Environmental Processes*, GeoPlanet: Earth and Planetary Sciences, Springer, Cham 2015, 229–254. DOI: 10.1007/978-3-319-17719-9_10.
- [27] BERTRAM H.U., *The Flow in Trapezoidal Channels with Extreme Slope Roughness*, Mitteilungen des Leichtweiss-Instituts für Wasserbau der Technische Universität Braunschweig, 1985, Heft 86 (in German).
- [28] KUBRAK J., NACHLIK E., *Hydraulic fundamentals for calculating river channel capacity*, Wydawnictwo SGGW, Warszawa 2003 (in Polish).
- [29] GUNAWAN B., *A Study of Flow Structures in a Two-Stage Channel Using Field Data. A Physical Model and Numerical Modelling*, PhD Thesis, The University of Birmingham, Birmingham 2010.
- [30] RICKERT K., *The Influence of Vegetation on Light Conditions and Flow Behavior in Watercourses*, Institute for Water Management, Hydrology, and Agricultural Water Engineering, University of Hannover, Hanover 1986 (in German).